

Evaluation of Reference Equations of State for Density Prediction in Regasified LNG Mixtures Using High-Precision Experimental Data

Daniel Lozano-Martín¹ · Dirk Tuma² · César R. Chamorro³

Received: 18 August 2025 / Accepted: 13 October 2025 © The Author(s) 2025

Abstract

This study evaluates the performance of three reference equations of state (EoS), AGA8-DC92, GERG-2008, and SGERG-88, in predicting the density of regasified liquefied natural gas (RLNG) mixtures. A synthetic nine-component RLNG mixture was gravimetrically prepared. High-precision density measurements were obtained using a single-sinker magnetic suspension densimeter over a temperature range of (250 to 350) K and pressures up to 20 MPa. The experimental data were compared with EoS predictions to evaluate their accuracy. AGA8-DC92 and GERG-2008 showed excellent agreement with the experimental data, with deviations within their stated uncertainty. In contrast, SGERG-88 exhibited significantly larger deviations for this RLNG mixture, particularly at low temperatures of (250 to 260) K, where discrepancies reached up to 3 %. Even at 300 K, deviations larger than 0.4 % were observed at high pressures, within the model's uncertainty, but notably higher than those of the other two EoSs. The analysis was extended to three conventional 11-component natural gas mixtures (labeled G420 NG, G431 NG, and G432 NG), previously studied by our group using the same methodology. While SGERG-88 showed reduced accuracy for the RLNG mixture, it performed reasonably well for these three mixtures, despite two of them have a very similar composition to the RLNG. This discrepancy is attributed to the lower CO₂ and N₂ content typical in RLNG mixtures, demonstrating the sensitivity of EoS performance to minor differences in composition. These findings highlight the importance of selecting appropriate EoS models for accurate density prediction in RLNG applications.

Keywords AGA8-DC92 · GERG-2008 · Gravimetric preparation · Regasified LNG · SGERG-88 · Single-sinker densimeter

Extended author information available on the last page of the article

Published online: 31 October 2025



1 Introduction

Natural gas plays a vital role in current energy policies and is projected to become even more significant in the near future. Several factors contribute to this anticipated growth, including its relatively low cost, reduced carbon dioxide emissions compared to other fossil fuels, and its compatibility with renewable alternatives, such as hydrogen and biomethane [1, 2]. These characteristics position natural gas as a key enabler in the ongoing transition toward a low-carbon energy system [3, 4].

Liquefied Natural Gas (LNG) enhances the flexibility of global natural gas markets by allowing for a broader diversification of supply sources and offering alternatives against potential supply disruptions [5]. Natural gas (NG) primarily consists of methane, along with varying amounts of other hydrocarbons—such as ethane, propane, butane, and pentane—and non-combustible compounds, often referred to as impurities, like carbon dioxide, water, and nitrogen [6]. NG composition depends on the source and process of extraction. The liquefaction of natural gas improves its transportability, making economically feasible to move large volumes over long distances [7]. However, during LNG transport, some heat entry into the storage tanks is inevitable. This causes a small portion of the LNG to evaporate, enriching the vapor phase with the more volatile components and changing the composition of the remaining liquid. The evaporated portion, known as boil-off gas, is often used as fuel by the LNG carrier itself [8]. As a result, Regasified Liquefied Natural Gas (RLNG) typically exhibits a slightly different composition than the original NG, with a higher concentration of heavier hydrocarbons and fewer impurities [9, 10].

For custody transfer and billing purposes, the accurate measurement of NG energy supplied is essential. Two main methodologies are employed to determine this value [11]. The first, known as the Gas Chromatography (GC) method, utilizes temperature, pressure, actual volumetric flow rate, and gas composition-determined via a process gas chromatographic analysis—as input parameters. Based on the gas composition, the higher heating value (HHV) can be calculated using the procedure defined in ISO 6976 [12]. The gas flow rate measured under flowing conditions must then be converted to standard conditions using appropriate equations of state (EoS), such as AGA8-DC92 [13] (referenced in ISO 12213-2 [14]) and GERG-2008 [15] (ISO 20765–2 [16]), which are widely adopted for this purpose.

The alternative approach, referred to as the Calorimetry Method (CM), also requires temperature, pressure, and actual volumetric flow rate as inputs. However, instead of relying on gas composition analysis, it employs the HHV obtained from an online calorimeter. The conversion of gas volume from flowing to standard conditions is performed using the SGERG-88 equation of state [17] (as specified in ISO 12213-3 [18]), which requires three of the following four parameters as inputs: HHV, relative density (also denoted as specific gravity, SG), and the individual concentrations of CO₂ and N₂. The CM method does not require a detailed composition analysis, as it treats the hydrocarbon content as an equivalent hydrocarbon mixture.

While the GC method is well-established and considered highly accurate, it also has some limitations. One among these is the relatively slow response time



of typical gas chromatographs, which, depending on the configuration of the setup, requires up to 10 min to produce a complete composition analysis, while flow meters provide flow measurements every second. The CM method offers a potential solution to this limitation and may serve as a viable alternative in natural gas energy metering systems, particularly with the advent of advanced calorimeters and their expanding role in the industry.

Currently, the AGA8-DC92 [13], GERG-2008 [15], and SGERG-88 [17] EoS are widely used by pipeline operators in both the USA and Europe for custody transfer and pipeline metering, as reported in various studies [19] and evidenced by their adoption in international standards [14, 16, 18]. These models have been developed using consolidated experimental data from pure substances and binary mixtures. However, their accuracy in predicting the behavior of ternary and more complex gas mixtures remains to be thoroughly validated. Therefore, further evaluation using high-quality experimental data is necessary which in turn requires the availability of highly accurate gas mixtures [3]. The primary objective of the present study is to assess and compare the performance of these three EoS in predicting the density of a RLNG mixture, which has been gravimetrically prepared to ensure minimal uncertainty in its composition.

To evaluate the performance of various reference equations of state (EoS) in predicting the density of regasified liquefied natural gas (RLNG) mixtures, a representative 9-component high-calorific natural gas mixture was prepared using gravimetric methods. The density of this mixture was measured with a single-sinker magnetic suspension densimeter (SSMSD) across a temperature range of (250 to 350) K and at pressures up to 20 MPa. The resulting experimental data were compared against three widely adopted reference EoS models in the natural gas industry: AGA8-DC92 [13], GERG-2008 [15], and SGERG-88 [17], all of which are commonly used for custody transfer and billing applications.

2 Theory and Calculation

The AGA8-DC92 model [13] was developed by the American Gas Association and is recognized as a standard for natural gas property calculations. Initially based on a virial expansion of the compressibility factor, it was later reformulated into an explicit Helmholtz energy framework to better capture both calorific and volumetric properties [20] following multiple revisions. Its currently validated range includes gas and supercritical phases between (250 and 350) K and pressures up to 30 MPa, with an estimated uncertainty in density for the temperature, pressure, and composition ranges considered in this work of 0.1 %.

The GERG-2008 EoS, developed by Kunz and Wagner [15] for the Groupe Européen de Recherches Gazières as an expansion of the GERG-2004 [21] EoS, extends the capabilities of AGA8-DC92 [13] by incorporating vapor-liquid equilibrium and liquid-phase behavior over a broader range of (60 to 700) K and pressures up to 70 MPa [16]. The GERG-2008 can model thermophysical properties of NG mixtures containing up to 21 components under pipeline conditions. Recent improvements of GERG-2008 have expanded its applicability in two important areas: (1)



LNG applications, through improved departure functions for binary mixtures containing methane, increasing its accuracy in the subcooled liquid region (90 K to 180 K, up to 10 MPa) [22–24] and (2) hydrogen-rich mixtures, by incorporating updated pure-component equations and improved binary interaction terms [25], supporting its use for hydrogen-enriched NG mixtures. Its estimated uncertainty in density for the temperature, pressure, and composition ranges considered in this work is 0.1 %.

Both AGA8-DC92 [13] and GERG-2008 [15] require a full compositional analysis of the gas mixture to reliably compute thermodynamic properties. In contrast, the SGERG-88 model [17], introduced in the 1997 release of ISO 12213-3 [18], uses a simplified input set consisting of any three parameters out of the higher heating value (HHV), relative density, and concentrations of CO₂ and N₂, plus mole fraction of H₂, at presence of H₂. SGERG-88 equation of state [26] is a virial-type thermal equation based on the Master (or Molar) GERG-88 virial equation [27]. Like all virial equations, it is only applicable in homogeneous gas phase, being adopted as a standard for the calculation of the compressibility factor, Z, of natural gas-like mixtures with an estimated uncertainty below 0.2 \% within the pressure and temperature ranges of (0 to 12) MPa and (263 to 338) K, respectively. The uncertainty increases to about 0.5 % for pressures between (12 and 16) MPa or for temperatures outside the aforementioned range and exceeds 0.5 % for pressures above 16 MPa [18]. Internally, the SGERG-88 EoS treats the natural gas mixture as a five-component mixture consisting of nitrogen, carbon dioxide, hydrogen, carbon monoxide, and an equivalent hydrocarbon (representing all the alkane hydrocarbons of the mixture as a single pseudo-component with the same thermodynamic properties). This model offers a more accessible approach for estimating gas properties when detailed compositional data are unavailable.

2.1 RLNG Mixture Preparation

A synthetic natural gas mixture composed of nine components, representative of a typical RLNG composition with high calorific value, was prepared at the Federal Institute for Materials Research and Testing (BAM, Berlin, Germany) in a 10 dm³ aluminum cylinder (Luxfer Gas Cylinders Inc., BAM cylinder no. 96054928–161019). The preparation followed the gravimetric method outlined in ISO 6142–1 [28] for reference materials, which ensures minimal uncertainty in the final composition. The mixture was prepared from high-purity individual gases through a series of intermediate pre-mixtures. Mass measurements along the entire filling procedure were performed using an electronic comparator balance (Sartorius LA 34000P-0CE) and a high-precision mechanical balance (Voland HCE 25), ensuring traceability and accuracy. After preparation, the gas mixture was homogenized by controlled rolling and heating. The final molar composition, x_i , together with the associated expanded (k=2) uncertainty in absolute terms, $U(x_i)$, is presented in Table 1.

Following homogenization, the mixture was shipped to the University of Valladolid (Valladolid, Spain). Prior to shipment, the composition was independently



Table 1 Composition of the RLNG mixture (cylinder no. 96054928–161019) studied in this work, with impurities compounds marked in italic type, and normalized composition without impurities

Component	Composition of the R	LNG mixture	Normalized comp RLNG mixture w	L .
	$10^2 x_i / (\text{mol·mol}^{-1})$	$10^2 U(x_i) / (\text{mol·mol}^{-1})$	$\frac{10^2 x_i}{\text{/ (mol \cdot mol^{-1})}}$	$10^2 U(x_i)$ / (mol·mol ⁻¹)
Methane	87.5790	0.0036	87.5791	0.0036
Nitrogen	0.11947	0.00015	0.11947	0.00015
Carbon Dioxide	0.020187	0.000082	0.020187	0.000082
Ethane	9.9437	0.0011	9.9437	0.0011
Propane	1.99856	0.00077	1.99857	0.00077
<i>n</i> -Butane	0.150132	0.000078	0.150132	0.000078
Isobutane	0.148984	0.000036	0.148984	0.000036
<i>n</i> -Pentane	0.019900	0.000024	0.019900	0.000024
Isopentane	0.020023	0.000024	0.020023	0.000024
Oxygen	0.000011	0.000009		
Hydrogen	0.000010	0.000005		
Carbon Monoxide	0.000001	0.000001		
Neopentane	0.000042	0.000021		
n-Hexane	0.0000005	0.0000004		
Propene	0.000002	0.000002		
Ethylene	0.0000015	0.0000013		
Nitric Oxide	0.000000001	0.000000001		

verified at BAM using gas chromatography (GC) on a Siemens MAXUM II multichannel process analyzer. The analysis employed a bracketing calibration method in accordance with ISO 12963 [29], using certified reference gases of appropriate composition and following the BAM certification protocol. Further methodological details are available in a previous work [30] and references cited therein.

The uncertainty in the mole fractions of each component was assessed using the law of propagation of uncertainty, as recommended by the Guide to the Expression of Uncertainty in Measurement [31]. This evaluation considered the purity of the source gases and the entire preparation process. The agreement between the gravimetric and chromatographic compositions was within the acceptance limits defined by BAM, thereby the validation equals a successful certification of the mixture.

2.2 Experimental Setup and Procedure

Density measurements were performed at the University of Valladolid using a single-sinker magnetic suspension densimeter (SSMSD), known for its high accuracy across wide temperature and pressure ranges. The system consists of a measuring cell filled with the sample gas, where a monocrystalline silicon sinker with a



precisely calibrated volume ($Vs = 226.4440 \pm 0.0026$ cm³ at ambient conditions) is suspended.

Density is determined based on Archimedes' principle, using the sinker's mass difference in vacuum and in the fluid, measured with a high-precision microbalance (XPE205DR, Mettler Toledo) via magnetic coupling:

$$\rho = \frac{(m_{S0} - m_{Sf})}{V_S(T, p)} \tag{1}$$

where m_{S0} is the "true" mass of the sinker weighed in the evacuated measuring cell, $m_{\rm Sf}$ is the "apparent" mass of the sinker weighed when the cell was filled with the fluid under study, and Vs(T,p) is the volume of the sinker at temperature T and pressure p.

The method, originally developed by Wagner's group at the University of Bochum, Germany [32-35], was adapted from two-sinker to single-sinker configurations [36, 37], maintaining high precision especially at elevated densities. The measurement procedure involves the use of two calibrated masses of titanium and tantalum of nearly the same volume and whose difference in mass, due to the big difference in density, approximates the mass of the sinker. The alternating use of these masses allows the balance to operate near zero and minimizes linearity errors.

Corrections for force transmission errors—both apparatus- and fluid-specific are applied. The apparatus-specific effect is determined by calculating the sinker weight in vacuum once all the data for an isotherm has been collected. This correction must always be applied to avoid significant errors [38]. The fluid-specific effect depends on the specific magnetic susceptibility of the fluid χ_s and on the so-called apparatus-specific constant ε_o , previously determined for our densimeter [39].

Pressure is monitored using two quartz transducers (Digiquartz 2300A-101 and Digiquartz 43KR-HHT-101, both from Paroscientific Inc.), with expanded (k=2)uncertainties of $U(p) = [6.0 \cdot 10^{-5} (p/\text{MPa}) + 2 \cdot 10^{-3}]$ MPa for the low-pressure transducer (0 to 3) MPa, and $U(p) = [7.5 \cdot 10^{-5} (p/\text{MPa}) + 4 \cdot 10^{-3}]$ MPa for the high-pressure transducer (3 to 20) MPa.

Temperature control is achieved via an oil thermal bath (Dyneo DD-1000F, Julabo GmbH) and an electrical heating cylinder with a temperature controller (MC-E, Julabo GmbH), with measurements taken using platinum resistance thermometers (SPRT-25, Minco Products Inc.) and an AC resistance bridge (ASL F700, Automatic Systems Laboratory), yielding an expanded (k=2) uncertainty U(T) = 0.015 K.

Further details on the experimental setup and methodology are displayed in prior publications [40, 41].

2.3 Experimental Uncertainty Budget

The overall expanded (k=2) uncertainty $U_{\rm T}(\rho_{\rm exp})$ for the experimental density measurements is summarized in Table 2, both in absolute and relative terms. This uncertainty incorporates contributions from the density determination itself, $U(\rho_{exp})$,



Source	Contribution $(k=2)$	Units	Estimation in dens	ity $(k=2)$
			kg·m ⁻³	%
Temperature, T	0.015	K	< 0.0027	< 0.0019
Pressure, p	< 0.005	MPa	0.023 to 0.097	0.016 to 0.37
Composition, x_i	< 0.0004	$\text{mol}\cdot\text{mol}^{-1}$	< 0.018	< 0.010
Density, ρ	0.024 to 0.051	$kg \cdot m^{-3}$	0.024 to 0.051	0.021 to 0.37

Table 2 Contributions to the expanded (k=2) overall uncertainty in density, $U_T(\rho_{\rm exp})$, for the RLNG mixture studied in this work

previously characterized for our SSMSD as a function of fluid density, $\rho_{\rm exp}$, and magnetic susceptibility, $\chi_{\rm s}$ [39, 41]:

$$U(\rho_{\rm exp})/({\rm kg\cdot m^{-3}}) = 2.5\cdot 10^4 \cdot \chi_s/({\rm m^3\cdot kg^{-1}}) + 1.1\cdot 10^{-4}\cdot \rho_{\rm exp}/({\rm kg\cdot m^{-3}}) + 2.3\cdot 10^{-2} \end{tabular} \tag{1}$$

Additional sources of uncertainty—pressure, u(p), temperature, u(T), and composition, $u(x_i)$ —were combined using the law of propagation of uncertainty [31]:

$$U_{\mathrm{T}}(\rho_{\mathrm{exp}}) = 2 \left[u(\rho_{\mathrm{exp}})^{2} + \left(\frac{\partial \rho}{\partial p} \Big|_{T,x} u(p) \right)^{2} + \left(\frac{\partial \rho}{\partial T} \Big|_{p,x} u(T) \right)^{2} + \sum_{i} \left(\frac{\partial \rho}{\partial x_{i}} \Big|_{T,p,x_{j} \neq x_{i}} u(x_{i}) \right)^{2} \right]^{0.5}$$
(3)

Partial derivatives of density with respect to pressure and temperature were estimated using REFPROP 10 [42], which employs the enhanced GERG-2008 EoS [22, 25]. A detailed description of the REFPROP software can be found in [43]. Among all contributors to the uncertainty budget, uncertainties from pressure and density measurements dominate, reaching up to 0.097 kg·m⁻³ (0.37 %). In contrast, uncertainties from composition and temperature are significantly lower, below 0.018 kg·m⁻³ (0.01 %) and 0.0027 kg·m⁻³ (0.002 %), respectively. The total expanded uncertainty ranges from (0.033 to 0.11) kg·m⁻³, corresponding to relative uncertainties between 0.027 % and 0.52 %.

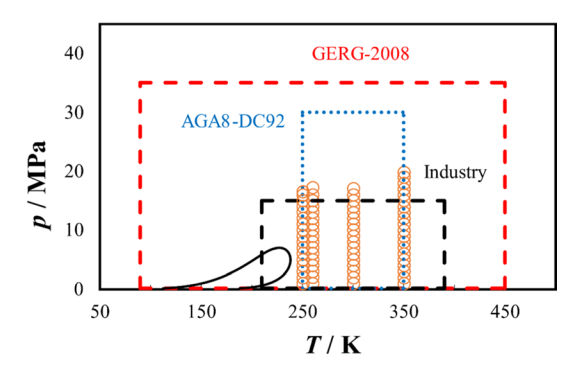
3 Results

Density measurements were recorded at four temperatures, (250, 260, 300, and 350) K, with pressure successively decreasing in 1 MPa steps from 20 MPa down to 1 MPa. Figure 1 presents the data points for the mixture, along with the saturation curve calculated from the GERG-2008 EoS [15], the typical operational ranges for pipeline conditions in the gas industry, and the approved application limits for both the AGA8-DC92 [13] and the GERG-2008 EoS models.

Table 3 presents the experimental (p, ρ, T) data for the RLNG mixture, along with the expanded uncertainty in density (k=2) calculated using Eq. 2, expressed in both absolute and percentage terms. It also includes the relative



Fig. 1 (p, T) phase diagram showing the experimental points measured (O) and the calculated phase envelope (solid line) using the GERG-2008 [15] EoS for the RLNG mixture. The marked temperature and pressure ranges represent the range of validity of the AGA8-DC92 [13] EoS (blue-dotted line) and GERG-2008 EoS (red-dashed line), and the area of interest for the gas industry (black-dashed line)



International Journal of Thermophysics

deviations of the experimental densities from those predicted by the AGA8-DC92 [13], GERG-2008 [15], and SGERG-88 [17] EoS. The densities predicted by AGA8-DC92 and GERG-2008 were obtained using the REFPROP 10 software [42], while those predicted by the SGERG-88 EoS were calculated using the GasCalc software [44]. It is worth noting that, in the case of the GasCalc software for the SGERG-88 EoS, the input variables used in this work are composition, temperature, and pressure. The software internally converts this set of variables into the natural variables required by the SGERG-88 EoS.

4 Discussion

4.1 Deviation Analysis of EoS for the RLNG Density Data

Figure 2 presents the percentage relative deviations of the experimental density data for the RLNG mixture from the values calculated using the AGA8-DC92 [13], GERG-2008 [15], and SGERG-88 [17] EoS. The density values predicted by the different EoS were calculated using the normalized, impurity-free composition provided in Table 1. The numerical values of these deviations are listed in the last three columns of Table 3.

The relative deviations between the experimental density data and the AGA8-DC92 [13] and GERG-2008 [15] EoS, shown in Fig. 2a and b, respectively, generally fall within the stated uncertainty of these models ($U(\rho_{EoS}) = 0.1$ %), except at the lower temperatures of (250 and 260) K and pressures between (5 and 15) MPa, where deviations can reach up to +0.20 %.

In contrast, the relative deviations between the experimental data and the SGERG-88 [17] EoS, shown in Fig. 2c, are larger approximately by one order of magnitude, in the limits, or above, the stated uncertainty of this model. At 250 K and pressures between (11 and 12) MPa, deviations can reach up to as much as + 3.0 %. At 260 K, deviations of up to + 1.8 % are observed at pressures between (12 and 13) MPa. Only at 300 K do the deviations remain within an



Table 3 Experimental (p, ρ_{exp}, T) measurements for the RLNG mixture, absolute and relative expanded (k=2) uncertainty in density, $U(\rho_{exp})$, relative deviations from the density given by the AGA8-DCO2 [13] FoS. ρ_{exp} , the GFRG-2008 [15] FoS. ρ_{exp} and the AGA8-DCO2 [13] FoS. ρ_{exp} and the AGA8-DCO2 [13] FoS. ρ_{exp} and the AGA8-DCO2 [13] FoS. ρ_{exp} are the GFRG-3008 [15] FoS. ρ_{exp} and the AGA8-DCO2 [13] FoS. ρ_{exp} are the GFRG-3008 [15] FoS. ρ_{exp} and the AGA8-DCO2 [13] FoS. ρ_{exp} are the GFRG-3008 [15] FoS.

VI / I	p / MFa ⁻	$\rho_{\rm exp} / ({\rm kg \cdot m^{-3}})^{\rm a}$	m^{-3}) ^a $U(\rho_{\rm exp}) / (kg \cdot m^{-3}) 10^2 U(\rho_{\rm exp}) / \rho_{\rm exp}$	$10^2 U(\rho_{\rm exp})/\rho_{\rm exp}$	10^{2}	10^{2}	10^{2}
		•	•		$(\rho_{\text{exp}} - \rho_{\text{AGA8-DC92}})/\rho_{\text{AGA8-DC92}}$	$(\rho_{\rm exp} - \rho_{\rm GERG-2008})/\rho_{\rm GERG-2008}$	$(\rho_{\exp} - \rho_{\text{SGERG-88}})/\rho_{\text{SGERG-88}}$
250 K							
250.184	16.593	250.095	0.051	0.021	0.050	0.011	1
250.183	16.044	245.491	0.051	0.021	0.057	600.0	1
250.183	15.047	236.195	0.050	0.021	0.072	0.008	1.8
250.181	14.033	225.238	0.049	0.022	0.088	0.013	2.3
250.182	13.038	212.578	0.047	0.022	0.109	0.029	2.7
250.182	12.040	197.504	0.045	0.023	0.140	0.051	3.0
250.182	11.027	179.357	0.043	0.024	0.174	0.076	2.9
250.184	10.026	158.582	0.041	0.026	0.174	0.114	2.6
250.184	9.021	135.812	0.038	0.028	0.153	0.171	2.1
250.182	8.015	112.955	0.036	0.032	0.150	0.193	1.7
250.184	7.012	91.783	0.033	0.036	0.158	0.173	1.3
250.182	800.9	73.078	0.031	0.043	0.136	0.125	1.0
250.183	5.006	56.832	0.029	0.052	0.102	0.087	0.74
250.183	4.008	42.734	0.028	0.065	0.062	0.059	0.52
250.181	2.996	30.155	0.026	0.087	0.030	0.044	0.33
250.183	2.003	19.158	0.025	0.131	0.020	0.045	0.20
250.186	1.003	9.151	0.024	0.261	0.036	0.059	0.12
260 K							
260.179	17.278	234.440	0.050	0.021	0.083	0.030	0.37
260.180	16.046	223.151	0.048	0.022	0.091	0.035	0.94
260.179	15.043	212.601	0.047	0.022	0.100	0.043	1.3
081.090	17.040	009 000	0.046	2000	0 117	2200	1.6



7 / K ^(a) p 260.178 13 260.178 13	p / MPa ^a	$a / (k \circ m^{-3})^a / (k \circ m^{-3}) 10^2 / (a) / a$	1110 110m-31	102 111, 11,	102	102	102
		L'exp. (exp.	O (vexp) / (wg III)	$10^{\circ} C(\rho_{\rm exp})/\rho_{\rm exp}$	10		10
			,		$(\rho_{\rm exp} - \rho_{\rm AGA8-DC92})/\rho_{\rm AGA8-DC92}$	$(\rho_{\rm exp} - \rho_{\rm GERG-2008})/\rho_{\rm GERG-2008})$	$(\rho_{\rm exp} - \rho_{\rm SGERG-88})/\rho_{\rm SGERG-88}$
	13.040	186.904	0.044	0.024	0.127	0.064	1.8
	12.041	171.432	0.042	0.025	0.135	0.078	1.8
260.179	11.021	153.931	0.040	0.026	0.134	0.106	1.6
260.179 10	10.026	135.646	0.038	0.028	0.120	0.125	1.3
260.177	9.021	116.864	0.036	0.031	0.117	0.133	1.0
260.178	8.014	209.86	0.034	0.035	0.119	0.125	0.83
260.178	7.010	81.648	0.032	0.039	0.114	0.108	0.65
260.176	6.011	66.280	0.030	0.046	0.094	0.086	0.50
260.175	5.010	52.388	0.029	0.055	0.066	0.064	0.37
260.176	4.007	39.846	0.027	690.0	0.041	0.050	0.26
260.173	3.004	28.510	0.026	0.092	0.023	0.043	0.18
260.174	2.004	18.211	0.025	0.137	0.017	0.042	0.11
260.180	1.003	8.752	0.024	0.273	0.036	0.058	0.08
300 K							
300.098	17.088	165.989	0.042	0.025	0.087	0.035	0.16
300.096	16.018	155.831	0.041	0.026	0.082	0.036	0.30
300.097	15.011	145.778	0.039	0.027	0.077	0.039	0.39
300.097 1	14.011	135.398	0.038	0.028	0.072	0.041	0.44
300.098	13.012	124.704	0.037	0.030	0.069	0.044	0.45
300.099	12.012	113.786	0.036	0.032	0.067	0.046	0.43
300.099	11.013	102.815	0.035	0.034	0.070	0.053	0.39
300.099	10.014	91.870	0.033	0.036	0.061	0.049	0.34
300.008	9.011	81.053	0.032	0.040	0.052	0.046	0.28
300.097	8.007	70.488	0.031	0.044	0.044	0.045	0.23



 $(\rho_{\rm exp} - \rho_{\rm SGERG-88})/\rho_{\rm SGERG-88}$ -0.73-0.49-0.40-0.32-0.25-0.20-0.16 -0.12-0.10-0.08-0.06-0.61-0.05-0.05 0.05 0.05 10^{2} $(\rho_{\rm exp} - \rho_{\rm GERG-2008})/\rho_{\rm GERG-2008}$ -0.008-0.003-0.009-0.010-0.009-0.007-0.007-0.002-0.0070.001 -0.001< 0.001 0.002 10^{2} $(\rho_{\exp} - \rho_{AGA8-DC92})/\rho_{AGA8-DC92}$ -0.019-0.002-0.010-0.016-0.023 -0.025 -0.019-0.022-0.020-0.0160.018 0.00 -0.021-0.0210.025 0.034 0.040 10^2 $\rho_{\rm exp} \, / \, ({\rm kg \cdot m^{-3}})^a \, \, \, U(\rho_{\rm exp}) \, / \, ({\rm kg \cdot m^{-3}}) \, \, \, 10^2 \, \, U(\rho_{\rm exp}) / \rho_{\rm exp}$ 0.318 0.034 0.036 0.038 **2.04** 0.048 0.028 0.029 0.030 0.033 0.161 0.031 0.041 0.038 0.038 0.036 0.035 0.034 0.033 0.033 0.032 0.030 0.028 0.026 0.025 0.0390.037 0.029 0.028 0.027 0.024 0.031 0.027 41.045 28.875 14.598 107.237 99.803 92.344 84.803 77.258 69.713 62.238 54.833 47.508 50.463 32.050 23.360 21.787 5.277 7.47 [able 3 (continued) p / MPa^a 1.002 9.013 8.017 17.012 5.009 3.010 2.009 1.008 0.005 900.6 8.007 7.006 5.004 4.003 2.002 6.014 4.006 2.990 300.008 300.008 300.102 350.095 350.096 350.098 350.100 350.099 350.098 350.099 350.098 350.098 350.098 350.098 350.098 300.097 350.095 350.094 350.094 $T/\mathrm{K}^{\mathrm{(a)}}$ 350 K



International Journal of Thermophysics

$\overline{}$
nec
n
Ξ.
ö
٣
m
<u>u</u>
9
₽

	((
$ \begin{array}{c ccccccccccccccccccccccccccccccccccc$	$T/K^{(a)}$	p / MPa ^a	ρ _{exp} / (kg·m	$(1^{-3})^a$ $U(\rho_{\rm ext})$	$_{\rm p}$) / (kg·m ⁻³) 10 ² $U(\rho_{\rm exp})/\rho_{\rm exp}$	10 ²	10^{2}		10 ²
$ \begin{array}{c ccccccccccccccccccccccccccccccccccc$			•			$(\rho_{\rm exp} - \rho_{\rm AGA8-DC92})'_{t}$	$^{\prime}_{AGA8\text{-DC92}}$ ($ ho_{\exp}$	$^{-} ho_{ m GERG-2008})/ ho_{ m GERG-2008}$	$(\rho_{\exp} - \rho_{\text{SGERG-88}})/\rho_{\text{SGERG-88}}$
$\begin{array}{cccccccccccccccccccccccccccccccccccc$	350.099	4.003	26.259	0.026		-0.012	0.0	002	-0.03
0.010 0.021 -0.004 0.046 0.054 0.054 0.04 $\cdot 10^{-6} \cdot \frac{p}{\text{MPa}} + 3.5 \cdot 10^{-3}; U(p < 3)/\text{MPa} = 60 \cdot 10^{-6} \cdot \frac{p}{\text{MPa}} + 1.7 \cdot 10^{-3}; U(T) = 15$		3.004	19.467	0.025		-0.004	0.0	600	-0.02
0.046 0.054 0.04		2.003	12.822	0.024	•	0.010	0.0	121	-0.004
$10^{-6} \cdot \frac{p}{\text{MPa}} + 3.5 \cdot 10^{-3}$; $U(p < 3)/\text{MPa} = 60 \cdot 10^{-6} \cdot \frac{p}{\text{MPa}} + 1.7 \cdot 10^{-3}$; $U(T) = 15$	350.102	1.003	6.342	0.024		0.046	0.0)54	0.04
	^a Expanded $\frac{U(\rho)}{r} = 2$	uncer 5×10^4	tainties $\frac{Z_S}{2} + 1.1$	$(k=2):$ $\times 10^{-4} \times$	$U(p > 3) / \text{MPa} = 75 \cdot 10^{-6} \cdot \frac{\rho}{10^{-3}} + 2.3 \times 10^{-2}$	$\frac{p}{MPa} + 3.5 \cdot 10^{-3}$;	U(p < 3)/MPa = 0	$50 \cdot 10^{-6} \cdot \frac{p}{\text{MPa}} + 1.7 \cdot 10$	U(T) = 15



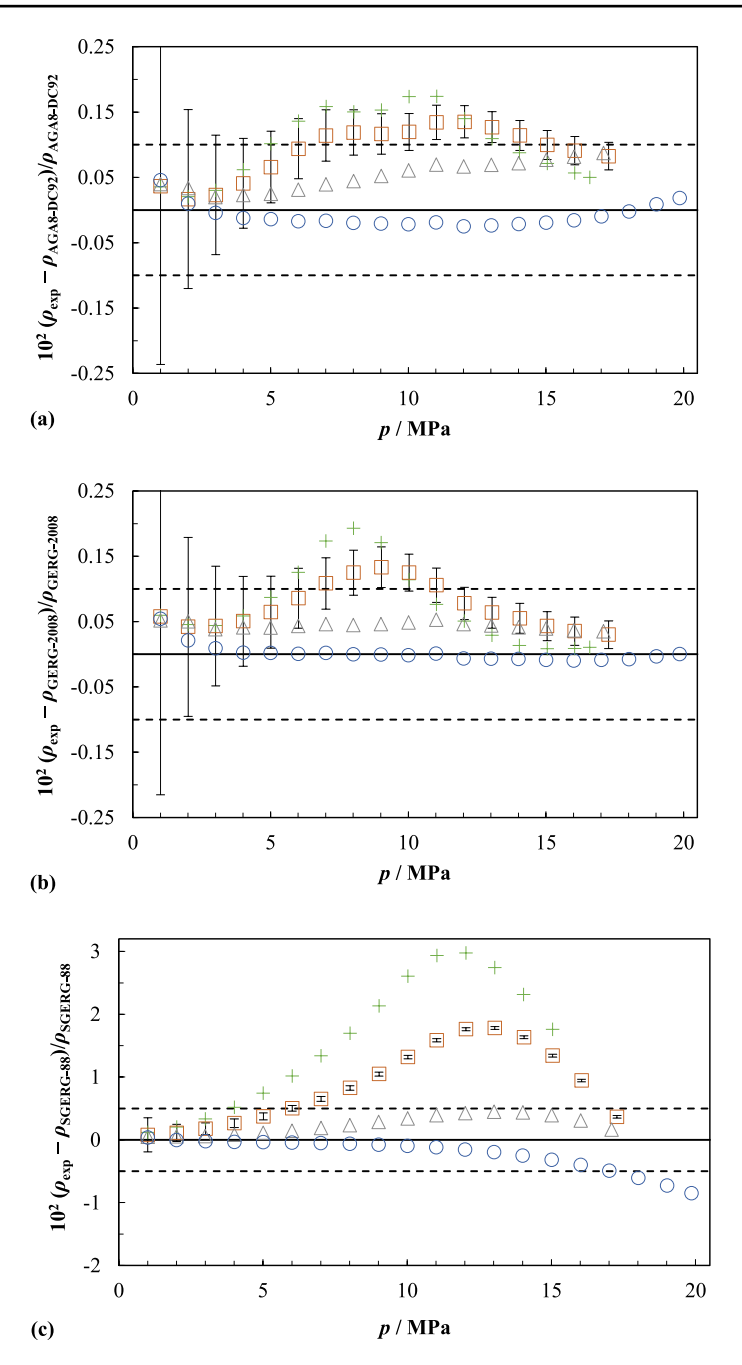


Fig. 2 Relative deviations in density of experimental $(p, \rho_{\rm exp}, T)$ data of RLNG mixture from density values calculated from (a) AGA8-DC92 [13] EoS, $\rho_{\rm AGA8-DC92}$ (b) GERG-2008 [15] EoS, $\rho_{\rm GERG-2008}$, and (c) SGERG-88 [17], $\rho_{\rm SGERG-88}$, as function of pressure for different temperatures: $+250~\rm K$, $\square 260~\rm K$, $\triangle 300~\rm K$, $\bigcirc 350~\rm K$. Dashed lines indicate the expanded (k=2) uncertainty of the corresponding EoS. Error bars on the 260 K dataset indicate the expanded (k=2) uncertainty of the experimental density. Note the different scale on the y-axis in plot (c)



200

uncertainty of 0.5 % across all pressures investigated. However, at the highest measured temperature of 350 K, deviations again exceed this limit at pressures above 17 MPa, showing negative deviations of up to -0.85 %.

4.2 Deviation Analysis of EoS for Other NG Density Data

Three natural gas (NG) mixtures were previously studied by our group using the same experimental technique, and the results have already been published. The compositions of these three mixtures, designated as G420 NG [30], G431 NG [45], and G432 NG [46], along with the composition of the RLNG mixture investigated in this work, are presented in Table 4. All four mixtures were prepared gravimetrically at BAM, ensuring minimal uncertainty in their compositions.

Table 4 also includes the molar mass M, normalized density ρ_n , relative density SG, higher heating value HHV, and Wobbe index W_s , for the four gas mixtures.

Table 4 Normalized, impurity-free composition of the RLNG mixture studied in this work, and of the other natural gas mixtures from our previous studies using the same experimental technique: G420 NG [30], G431 NG [45], and G432 NG [46]^(a), together with the molar mass M, normalized density ρ_n , relative density SG, higher heating value HHV, and Wobbe index W_s , for the four gas mixtures estimated using the REFPROP 10 software

Component	RLNG	G420 NG	G431 NG	G432 NG
	$10^2 x_i / (\text{mol·mol}^{-1})$	$10^2 x_i / (\text{mol·mol}^{-1})$	$10^2 x_i / (\text{mol·mol}^{-1})$	$\frac{10^2 x_i}{\text{/ (mol · mol^{-1})}}$
Methane	87.5790	87.6639	97.2362	85.0063
Nitrogen	0.11947	4.3215	1.40097	0.9508
Carbon dioxide	0.020187	1.62267	0.36146	1.44823
Ethane	9.9437	4.2252	0.398705	8.99177
Propane	1.99856	1.04900	0.201221	3.00256
<i>n</i> -Butane	0.150132	0.212726	0.100398	0.19994
Isobutane	0.148984	0.210383	0.100431	0.200443
<i>n</i> -Pentane	0.019900	0.051811	0.100853	0.100089
Isopentane	0.020023	0.052238	0.049928	0.049929
<i>n</i> -Hexane	_	0.052611	0.049883	0.049965
Oxygen	_	0.537990	_	_
Property	RLNG	G420 NG	G431 NG	G432 NG
Molar mass, M / (g/ mol)	18.166	18.260	16.628	18.954
Normalized density, $\rho_{\rm n}$ / (kg·m ⁻³)	0.77034	0.77400	0.70468	0.80379
Relative density, SG	0.629	0.632	0.575	0.656
Higher heating value, HHV / (MJ·m ⁻³)	42.003	37.678	37.749	41.726
Wobbe index W_s / $(MJ \cdot m^{-3})$	52.979	47.411	49.783	51.523

^aThe uncertainties of the NG mixtures are given in the corresponding references



These properties were estimated using the REFPROP 10 software [42] based on the normalized, impurity-free compositions and under reference conditions of 288.15 K and 0.101325 MPa. Based on these values, all four mixtures can be classified as high-calorific natural gases (H-Gas). According to the European standard EN 437 [47], H-Gas mixtures are defined as those with a Wobbe index between 47.2 and 54.7 MJ·m⁻³ and a relative density (SG, defined as the gas density relative to air) between 0.55 and 0.75.

The G420 NG mixture is an 11-component natural gas with a methane content comparable to that of the RLNG mixture, but with lower ethane and propane contents and higher concentrations of N_2 and CO_2 than the RLNG mixture. Densities were measured at five different temperatures (260, 275, 300, 325, and 350) K and up to a maximum pressure of 20 MPa. The G431 NG mixture is a 10-component natural gas primarily composed of methane (>97 %), but, again, with higher N_2 and CO_2 contents than the RLNG mixture. Densities were measured at five different temperatures (250, 275, 300, 325, and 350) K and up to a maximum pressure of 20 MPa. The G432 NG mixture is also a 10-component natural gas, with methane, ethane, and propane contents similar to those of the RLNG mixture; however, it also contains significantly higher amounts of N_2 and CO_2 than the RLNG mixture. Densities were measured at five different temperatures (260, 275, 300, 325, and 350) K and up to a maximum pressure of 20 MPa.

Figures 3, 4, and 5 show the percentage relative deviations of the experimental density data from the values calculated using the AGA8-DC92 [13], GERG-2008 [15], and SGERG-88 [17] EoS for the G420 NG, G431 NG, and G432 NG mixtures, respectively. Comparisons with the AGA8-DC92 and GERG-2008 EoS were previously analyzed in earlier publications (G420 NG [30], G431 NG [45], and G432 NG [46]), and are included here for completeness. The comparison with the SGERG-88 EoS represents a new contribution of this work. Table 5 provides a statistical comparison of the experimental density data for the three natural gas mixtures, G420 NG, G431 NG, and G432 NG, relative to the three EoS models, along with the corresponding statistical values for the RLNG mixture.

In Table 5, the statistical indicators are defined as follows: AARD (average absolute value of the relative deviations), ASRD (average signed relative deviation), and MaxARD (maximum absolute value of the relative deviation), as given by Eqs. (4) to (6):

AARD =
$$\frac{1}{N} \sum_{i=1}^{N} \left| 10^2 \frac{\rho_{i,exp} - \rho_{i,EoS}}{\rho_{i,EoS}} \right|$$
 (4)

ASRD =
$$\frac{1}{N} \sum_{i=1}^{N} \left(10^2 \frac{\rho_{i,exp} - \rho_{i,EoS}}{\rho_{i,EoS}} \right)$$
 (5)

$$MaxARD = max \left| 10^2 \frac{\rho_{i,exp} - \rho_{i,EoS}}{\rho_{i,EoS}} \right|$$
 (6)



200

Fig. 3 Relative deviations in density of experimental $(p, \rho_{\rm exp}, T)$ data of G420 NG [30] mixture from \blacktriangleright density values calculated from (a) AGA8-DC92 [13] EoS, $\rho_{AGA8-DC92}$, (b) GERG-2008 [15] EoS, $\rho_{\rm GERG-2008}$, and (c) SGERG-88 [17], $\rho_{\rm SGERG-88}$, as function of pressure for different temperatures: 260 K, \Diamond 275 K, \Diamond 300 K, \times 325 K, \bigcirc 350 K. Dashed lines indicate the expanded (k=2) uncertainty of the corresponding EoS. Error bars on the 260 K dataset indicate the expanded (k=2) uncertainty of the experimental density. Note the different scale on the y-axis in plot (c)

International Journal of Thermophysics

The density values given by the different EoS were calculated using the normalized composition without impurities given in Table 4.

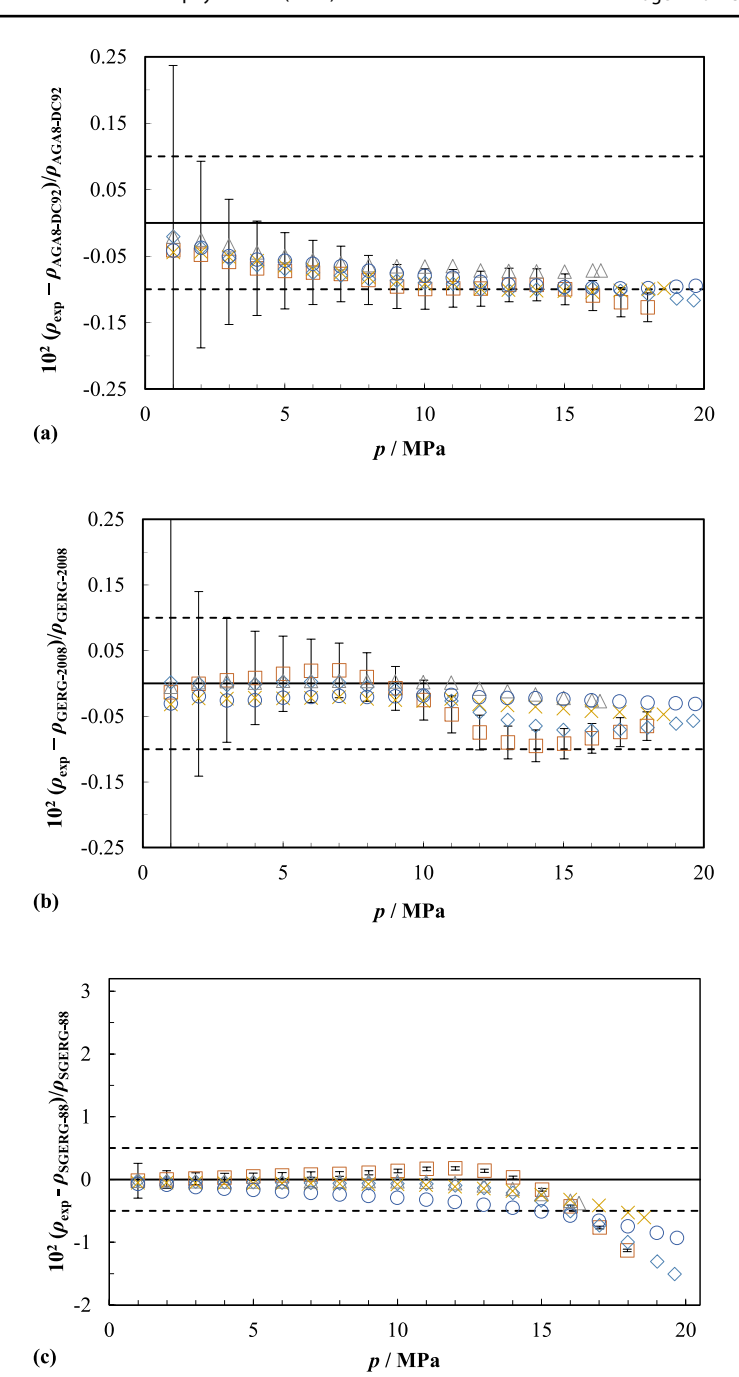
Figure 3a and b shows the relative deviations between the experimental density data for the G420 NG mixture and the AGA8-DC92 [13] and GERG-2008 [15] EoS, respectively. Both models provide an excellent representation of the experimental data, with most values falling within their stated uncertainty limits, even at the lowest temperature considered in this study, i.e., 260 K (instead of the typical 250 K). Only three data points, at 260 K and pressures above 15 MPa, exhibit deviations exceeding – 0.1 %. A comparison of the two models reveals that GERG-2008 performs slightly better (AARD of 0.027 %) than AGA8-DC92 (AARD of 0.078 %). The SGERG-88 [17] EoS shows lower accuracy, with an AARD of 0.23 % and a MaxARD of 1.51 %. Nevertheless, the largest part of the experimental data remains within the stated uncertainty of the SGERG-88 EoS, except at pressures above 15 MPa where experimental data show negative deviations, as illustrated in Fig. 3c.

Figures 4 and 5 display the relative deviations between the experimental density data and the three EoS models used for comparison for the G431 NG and G432 NG mixtures, respectively. The behavior observed is very similar to that previously discussed for the G420 NG mixture in Fig. 3. Both the AGA8-DC92 [13] and GERG-2008 [15] EoS perform very well in describing the experimental data, particularly for the G431 NG mixture, which has the highest methane content. For this mixture, the AARD values are 0.012 % for AGA8-DC92 and 0.032 % for GERG-2008. Only a few data points for the G432 NG mixture, at the lowest temperature of 250 K, show deviations exceeding the stated uncertainty of the EoS. The SGERG-88 [17] EoS again demonstrates slightly lower performance, with AARD values of 0.30 % for G431 NG and 0.18 % for G432 NG, and MaxARD values of 1.61 % and 1.16 %, respectively. Nonetheless, most of the experimental data are still captured within the uncertainty bounds of the SGERG-88 EoS, except at pressures above 15 MPa, where experimental data display again negative deviations, as shown in Figs. 4c and 5c.

The performance of the AGA8-DC92 [13] and GERG-2008 [15] EoS has also been evaluated by other authors for various natural gas mixtures. For instance, Farzaneh-Gord et al. [48] compared the AGA8-DC92 and GERG-2008 EoS for five typical Iranian natural gas compositions. Their study demonstrated that GERG-2008 consistently outperformed AGA8-DC92 across the entire range of pressures and temperatures considered. Notably, none of the mixtures studied was of the RLNG type. The results also indicated that GERG-2008 tends to predict higher compressibility factors than AGA8-DC92 in the practical measurement range.

Ahmadi et al. [49] simultaneously measured the density and speed of sound of a synthetic natural gas mixture (~88 mol-% methane) These measurements were carried out along five isotherms at temperatures between (323 and 415) K and pressures







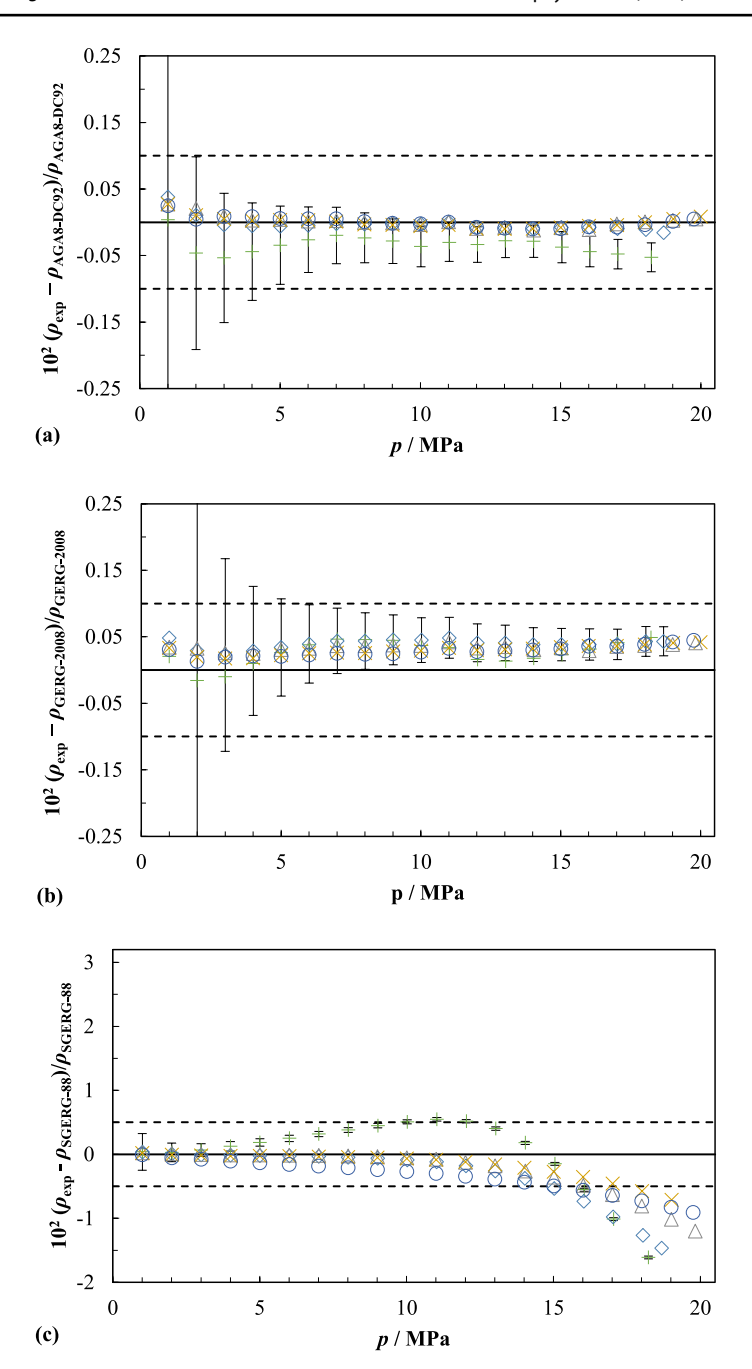


Fig. 4 Relative deviations in density of experimental $(p, \rho_{\rm exp}, T)$ data of G431 NG [45] mixture from density values calculated from (a) AGA8-DC92 [13] EoS, $\rho_{\rm AGA8-DC92}$, (b) GERG-2008 [15] EoS, $\rho_{\rm GERG-2008}$, and (c) SGERG-88 [17], $\rho_{\rm SGERG-88}$, as function of pressure for different temperatures: +250 K, \Diamond 275 K, \Diamond 300 K, \times 325 K, \bigcirc 350 K. Dashed lines indicate the expanded (k=2) uncertainty of the corresponding EoS. Error bars on the 250 K dataset indicate the expanded (k=2) uncertainty of the experimental density. Note the different scale on the y-axis in plot (c)



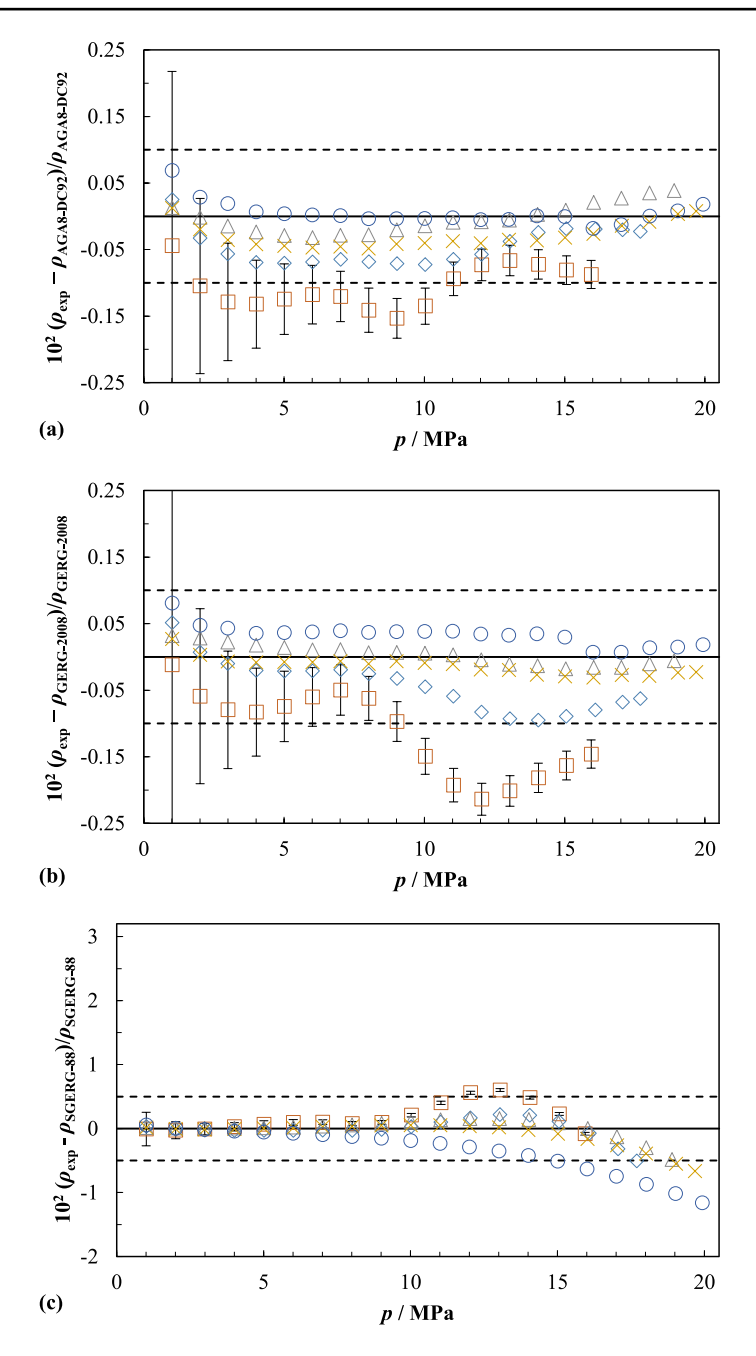


Fig. 5 Relative deviations in density of experimental $(p, \rho_{\rm exp}, T)$ data of G432 [46] NG mixture from density values calculated from (a) AGA8-DC92 [13] EoS, $\rho_{\rm AGA8-DC92}$, (b) GERG-2008 [15] EoS, $\rho_{\rm GERG-2008}$, and (c) SGERG-88 [17], $\rho_{\rm SGERG-88}$, as function of pressure for different temperatures: \Box 260 K, \Diamond 275 K, \triangle 300 K, \times 325 K, \bigcirc 350 K. Dashed lines indicate the expanded (k=2) uncertainty of the corresponding EoS. Error bars on the 260 K dataset indicate the expanded (k=2) uncertainty of the experimental density. Note the different scale on the y-axis in plot (c)



Table 5 Statistical analysis of the (p, p, T) dataset with respect to AGA8-DC92 [13], GERG-2008 [15], and SGERG-88 [17] EoS for the RLNG mixture studied in this

work, and	for oth	er natural gas	s mixtures	(G420 NG [30], G431 NG [work, and for other natural gas mixtures (G420 NG [30], G431 NG [45], and G432 NG [46]) from the literature	NG [46]) from	the literature				
Reference	$N^{(a)}$	Reference N(a) Covered ranges	səgı	Experimenta	Experimental vs AGA8-DC92EoS	C92EoS	Experimental vs GERG-2008 EoS	l vs GERG-2	008 EoS	Experimental vs SGERG-88 EoS	vs SGERG-	38 EoS
		T/K	<i>p /</i> MPa	AARD (%)	ASRD (%)	MaxARD (%)	AARD (%)	ASRD (%)	$\begin{array}{cccccccccccccccccccccccccccccccccccc$	AARD (%)	ASRD (%)	MaxARD (%)
RLNG	69	RLNG 69 250 to 350	1 to 20 0.063	0.063	0.056	0.17	0.048	0.046	0.19	99.0	0.55	2.98
G420 NG	100	3420 NG 100 260 to 350	1 to 20	0.078	-0.078	0.13	0.027	-0.025	0.095	0.24	-0.22	1.51
G431 NG	96	G431 NG 96 250 to 350	1 to 20	0.012	-0.007	0.054	0.032	0.032	0.049	0.30	-0.22	1.61
G432 NG	93	G432 NG 93 260 to 350	1 to 20	0.040	-0.033	0.15	0.043	-0.023	0.21	0.18	-0.07	1.16

AARD average absolute value of relative deviation, ASRD average signed relative deviation, MaxARD maximum absolute value of relative deviation ^aNumber of experimental points



up to the remarkably high value of 56 MPa. The experimental results showed good agreement with the predictions of both the AGA8-DC92 [13] and GERG-2008 [15] EoS.

The GERG-2008 [15] EoS was compared with the cubic equations of Peng–Robinson and Redlich–Kwong–Soave and the equation of state of Lee–Kesler–Plöcker for the representation of thermodynamic properties of natural gas in another study [9]. The EoS showed high potential for accurate process modeling.

In another study, Chaczykowski [19] analyzed the performance of the SGERG-88 [17] and AGA8-DC92 [13] EoS for a nine-component natural gas mixture with a methane content greater than 98 mol-%. The results indicated that both models yielded similar predictions.

5 Conclusion

A nine-component synthetic natural gas mixture, representative of typical RLNG, was prepared in reference quality with minimal uncertainty in composition at the Federal Institute for Materials Research and Testing (BAM, Berlin, Germany). High-precision experimental density measurements for this mixture were obtained using a single-sinker magnetic suspension densimeter (SSMSD) at the University of Valladolid (Valladolid, Spain). The experimental densities were compared with the densities calculated from three equations of state (EoS) commonly used in the natural gas industry: AGA8-DC92 [13], GERG-2008 [15], and SGERG-88 [17]. This comparison was also analyzed for three other NG mixtures, G420 NG, G431 NG, and G432 NG, previously measured using the same experimental technique by our group.

Both the AGA8-DC92 [13] and GERG-2008 [15] EoS demonstrated an excellent agreement with experimental data for the RLNG mixture and for the G420 NG, G431 NG, and G432 NG mixtures. The SGERG-88 [17] EoS showed a slightly lower accuracy for the three NG mixtures, but still within its stated uncertainty, but it failed to accurately predict the density of the RLNG mixture at the lowest temperatures studied (250 and 260) K, where deviations of up to +3 % were observed. Even at near-ambient conditions (e.g., 300 K), deviations reached up to +0.4 % at pressures between (11 and 15) MPa, within the claimed uncertainty of the SGERG-88 EoS, but nearly one order of magnitude greater than those observed for the other two EoS.

The compositions of the G420 NG, G431 NG, and G432 NG differ considerably in methane content, ranging from 87.7 mol-% in G420 NG to 97.2 mol-% in G431 NG, and in the combined ethane and propane content, ranging from 0.6 mol-% in G431 NG to 12.0 mol-% in G432 NG. Nevertheless, the SGERG-88 [17] EoS shows a similar predictive capacity for all three mixtures. It is worth noting that, despite the apparent similarity in composition between RLNG and G432 NG (similar combined ethane and propane content, i.e., around 12 mol-%) and between RLNG and G420 NG (similar methane content, i.e., around 87.6 mol-%), the capacity of the SGERG-88 EoS to predict their densities differs significantly. While the densities of G432 NG and G420 NG were well represented by the SGERG-88, the RLNG densities at low temperatures



showed considerable deviations from the predicted values. The main difference between these mixtures lies in their CO₂ and N₂ contents, as RLNG typically contains lower concentrations of both components. The CO₂ content in RLNG mixtures is generally below 0.2 mol-\%, often in the range of (0.01 to 0.1) mol-\%, and N₂ is typically below 1 mol-%, often around (0.1 to 0.5) mol-%. This characteristic is clearly reflected in the RLNG mixture, but not in the G420 NG, G431 NG, and G432 NG mixtures, which contain more than 0.3 mol-\% of CO₂ and more than 0.95 mol-\% of N₂. These composition differences may explain the discrepancies observed in density predictions by the SGERG-88 EoS.

International Journal of Thermophysics

Supplementary Information The online version contains supplementary material available at https://doi. org/10.1007/s10765-025-03669-4.

Acknowledgments This work represents the final experimental contribution utilizing the SSMSD at the University of Valladolid under the supervision of C.R. Chamorro. He extends his heartfelt gratitude to all coauthors of the 20 publications featuring high-precision density data for binary and multicomponent mixtures over the past two decades. Special thanks are due to Professor M.A. Villamañán for providing the opportunity to embark on this research journey, to the late Professor W. Wagner (†2024) and his team at the Ruhr-University of Bochum RUB, Germany, who generously hosted him in 1996 and introduced him to the fundamentals of this technique, and to his doctoral students M.E. Mondéjar (†2021), R. Hernández-Gómez, and D. Lozano-Martín for their dedication and invaluable collaboration.

Author contributions D.L-M. contributed to data curation, formal analysis, investigation, and writing review and editing. D.T. contributed to data curation, formal analysis, investigation, resources, and writing—review and editing. C.R.C. contributed to investigation, methodology, resources, supervision, writing-original draft, and writing-review and editing.

Funding Open access funding provided by FEDER European Funds and the Junta de Castilla y León under the Research and Innovation Strategy for Smart Specialization (RIS3) of Castilla y León 2021-2027. This study was supported by the Regional Government of Castilla y León (Junta de Castilla y León), the Ministry of Science and Innovation MCIN, the European Union NextGenerationEU/PRTR, under project C17.I01.P01.S21, and by the European Metrology Program for Innovation and Research (EMPIR), Funder ID:https://doi.org/10.13039/100014132, Grant No. 19ENG03 MefHySto.

Data Availability Data are provided within the manuscript or supplementary information files.

Declarations

Conflict of interest The authors have no competing interests to declare that are relevant to the content of this article.

Open Access This article is licensed under a Creative Commons Attribution 4.0 International License, which permits use, sharing, adaptation, distribution and reproduction in any medium or format, as long as you give appropriate credit to the original author(s) and the source, provide a link to the Creative Commons licence, and indicate if changes were made. The images or other third party material in this article are included in the article's Creative Commons licence, unless indicated otherwise in a credit line to the material. If material is not included in the article's Creative Commons licence and your intended use is not permitted by statutory regulation or exceeds the permitted use, you will need to obtain permission directly from the copyright holder. To view a copy of this licence, visit http://creativecommons.org/ licenses/by/4.0/.



References

- S.V.A. de Franco, D. da Cunha Ribeiro, A.P. Meneguelo, A comprehensive approach to evaluate feed stream composition effect on natural gas processing unit energy consumption. J. Nat. Gas Sci. Eng. 83, 3607 (2020). https://doi.org/10.1016/j.jngse.2020.103607
- M. Wang, R. Khalilpour, A. Abbas, Thermodynamic and economic optimization of LNG mixed refrigerant processes. Energy Convers. Manag. 88, 947–961 (2014). https://doi.org/10.1016/j.encon man.2014.09.007
- S.Z.S. Al Ghafri, F. Jiao, T.J. Hughes, A. Arami-Niya, X. Yang, A. Siahvashi, A. Karimi, E.F. May, Natural gas density measurements and the impact of accuracy on process design. Fuel 304, 121395 (2021). https://doi.org/10.1016/j.fuel.2021.121395
- Y. Hupka, I. Popova, B. Simkins, T. Lee, A review of the literature on LNG: hubs development, market integration, and price discovery. J. Commod. Mark. 31, 100349 (2023). https://doi.org/10. 1016/j.jcomm.2023.100349
- V. Vivoda, Lng import diversification and energy security in Asia. Energy Policy 129, 967–974 (2019). https://doi.org/10.1016/j.enpol.2019.01.073
- T.-V. Nguyen, B. Elmegaard, Assessment of thermodynamic models for the design, analysis and optimisation of gas liquefaction systems. Appl. Energy 183, 43–60 (2016). https://doi.org/10.1016/j. apenergy.2016.08.174
- X. Xiao, M. Richter, E.F. May, Isobaric heat capacities of liquefied natural gas (LNG) mixtures by differential scanning calorimetry at temperatures from 116 K to 150 K and pressures up to 6.90 MPa. Fuel 381, 132947 (2025). https://doi.org/10.1016/j.fuel.2024.132947
- B. Shingan, N. Banerjee, M. Kumawat, P. Mitra, V. Parthasarthy, V. Singh, Liquefied natural gas value chain: a comprehensive review and analysis. Chem. Eng. Technol. 47, 430–447 (2024). https://doi.org/10.1002/ceat.202300304
- F. Dauber, R. Span, Modelling liquefied-natural-gas processes using highly accurate property models. Appl. Energy 97, 822–827 (2012). https://doi.org/10.1016/j.apenergy.2011.11.045
- H. Uwitonze, S. Han, C. Jangryeok, K.S. Hwang, Design process of LNG heavy hydrocarbons fractionation: low LNG temperature recovery. Chem. Eng. Process. Process Intensif. 85, 187–195 (2014). https://doi.org/10.1016/j.cep.2014.09.002
- P. Zhang, L. Zhou, W. Xu, Compressibility factor calculation from gross calorific value and relative density for natural gas energy measurement. Int. J. Energy Res. 46, 9948–9959 (2022). https://doi. org/10.1002/er.7772
- International Organization for Standardization. ISO 6976. Natural gas Calculation of calorific values, density, relative density and Wobbe index from composition. Genève: 2016.
- Transmission Measurement Committee. AGA Report No. 8 Part 1 Thermodynamic Properties of Natural Gas and Related Gases DETAIL and GROSS Equations of State. Washington DC: 2017.
- International Organization for Standardization. ISO 12213-2. Natural gas Calculation of compression factor Part 2: Calculation using molar-composition analysis. Genève: 2006.
- O. Kunz, W. Wagner, The GERG-2008 wide-range equation of state for natural gases and other mixtures: an expansion of GERG-2004. J. Chem. Eng. Data 57, 3032–3091 (2012). https://doi.org/10. 1021/je300655b
- International Organization for Standardization. ISO 20765-2. Natural gas—Calculation of thermodynamic properties—Part 2: Single-phase properties (gas, liquid, and dense fluid) for extended ranges of application. Genève: 2015.
- M. Jaeschke, S. Audibert, P. van Caneghem, A.E. Humphreys, R. Janssen-van Rosmalen, Q. Pellei, J.A. Schouten, J.P.J. Michels, Simplified GERG Virial Equation for Field Use. SPE Prod. Eng. 6, 350–356 (1991). https://doi.org/10.2118/17767-PA
- International Organization for Standardization. ISO 12213–3. Natural gas Calculation of compression factor Part 3: Calculation using physical properties. Genève: 2006.
- M. Chaczykowski, Sensitivity of pipeline gas flow model to the selection of the equation of state.
 Chem. Eng. Res. Des. 87, 1596–1603 (2009). https://doi.org/10.1016/j.cherd.2009.06.008
- International Organization for Standardization. ISO 20765–1. Natural gas Calculation of thermodynamic properties Part 1: Gas phase properties for transmission and distribution applications.

 Genève: 2005
- Kunz O, Klimeck R, Wagner W, Jaeschke M. The GERG-2004 Wide-Range Equation of State for Natural Gases and Other Mixtures. Düsseldorf: 2007.



200

22. M. Thol, M. Richter, E.F. May, E.W. Lemmon, R. Span, EOS-LNG: a fundamental equation of state for the calculation of thermodynamic properties of liquefied natural gases. J. Phys. Chem. Ref. Data 48, 1-36 (2019). https://doi.org/10.1063/1.5093800

International Journal of Thermophysics

- 23. R. Lentner, P. Eckmann, R. Kleinrahm, R. Span, M. Richter, Density measurements of seven methane-rich binary mixtures over the temperature range from (100 to 180) k at pressures up to 9.7 MPa. J. Chem. Thermodyn. (2020). https://doi.org/10.1016/j.jct.2019.106002
- 24. R. Lentner, M. Richter, R. Kleinrahm, R. Span, Density measurements of liquefied natural gas (LNG) over the temperature range from (105 to 135) K at pressures up to 8.9 MPa. J. Chem. Thermodyn. 112, 68-76 (2017). https://doi.org/10.1016/j.jct.2017.04.002
- 25. R. Beckmüller, M. Thol, I.H. Bell, E.W. Lemmon, R. Span, New equations of state for binary hydrogen mixtures containing methane, nitrogen, carbon monoxide, and carbon dioxide. J. Phys. Chem. Ref. Data 50, 1–22 (2021). https://doi.org/10.1063/5.0040533
- 26. Jaeschke M, Humphreys AE. Standard GERG virial equation for field use Simplification of the Input Data Requirements for the GERG Virial Equation - an Alternative Means of Compressibility Factor Calculation for Natural Gases and Similar Mixtures. GERG Tech Monogr TM5 1991.
- 27. Jaeschke M, Audibert S, van Canegham P, Humphreys AE, Janssen-van Rosemalen R, Pellei Q, Michels JPJ, Schouten JA, ten Seldam CA. High Accuracy Compressibility Factor Calculation of Natural Gases and Similar Mixtures by Use of a Truncated Virial Equation. GERG Tech Monogr TM2 1989.
- 28. International Organisation for Standardization. ISO 6142-1. Gas analysis Preparation of calibration gas mixtures - Part 1: Gravimetric method for Class I mixtures. 2014.
- International Organization for Standardization. ISO 12963. Gas analysis Comparison methods for the determination of the composition of gas mixtures based on one- and two-point calibration. Genève: 2017.
- 30. R. Hernández-Gómez, D. Tuma, D. Lozano-Martín, C.R. Chamorro, Accurate experimental (p, ρ, T) data of natural gas mixtures for the assessment of reference equations of state when dealing with hydrogen-enriched natural gas. Int. J. Hydrogen Energy 43, 21983–21998 (2018). https://doi.org/10. 1016/i.iihvdene.2018.10.027
- 31. Joint Committee for Guides in Metrology (JCGM). GUM1995. Evaluation of measurement data -Guide to the expression of uncertainty in measurement. JCGM 100:2008. GUM 1995 with minor corrections, 2008.
- R. Kleinrahm, W. Wagner, Measurement and correlation of the equilibrium liquid and vapour densities and the vapour pressure along the coexistence curve of methane. J. Chem. Thermodyn. 18, 739–760 (1986). https://doi.org/10.1016/0021-9614(86)90108-4
- 33. H.W. Lösch, R. Kleinrahm, W. Wagner, Neue Magnetschwebewaagen für gravimetrische Messungen in der Verfahrenstechnik. Chem. Ing. Tech. 66, 1055-1058 (1994). https://doi.org/10.1002/cite. 330660808
- 34. X. Yang, R. Kleinrahm, M.O. McLinden, M. Richter, The magnetic suspension balance: 40 years of advancing densimetry and sorption science. Int. J. Thermophys. 44, 169 (2023), https://doi.org/10. 1007/s10765-023-03269-0
- 35. W. Wagner, R. Kleinrahm, Densimeters for very accurate density measurements of fluids over large ranges of temperature, pressure, and density. Metrologia 41, S24-39 (2004). https://doi.org/10.1088/ 0026-1394/41/2/S03
- 36. W. Wagner, K. Brachthäuser, R. Kleinrahm, H.W. Lösch, A new, accurate single-sinker densitometer for temperatures from 233 to 523 K at pressures up to 30 MPa. Int. J. Thermophys. 16, 399-411 (1995). https://doi.org/10.1007/BF01441906
- 37. J. Klimeck, R. Kleinrahm, W. Wagner, An accurate single-sinker densimeter and measurements of the (p, ρ, T) relation of argon and nitrogen in the temperature range from (235 to 520) K at pressures up to 30 MPa. J. Chem. Thermodyn. **30**, 1571–1588 (1998)
- 38. M.O. McLinden, R. Kleinrahm, W. Wagner, Force transmission errors in magnetic suspension densimeters. Int. J. Thermophys. 28, 429-448 (2007). https://doi.org/10.1007/s10765-007-0176-0
- D. Lozano-Martín, M.E. Mondéjar, J.J. Segovia, Determination of the force transmission error in a single-sinker magnetic suspension densimeter due to the fluid-specific effect and its correction for use with gas mixtures containing oxygen. Measurement (2020). https://doi.org/10.1016/j.measu rement.2019.107176. (Chamorro CR)
- 40. C.R. Chamorro, J.J. Segovia, M.C. Martín, M.A. Villamañán, J.F. Estela-Uribe, J.P.M. Trusler, Measurement of the (pressure, density, temperature) relation of two (methane+nitrogen) gas mixtures at temperatures between 240 and 400K and pressures up to 20MPa using an accurate



- single-sinker densimeter. J. Chem. Thermodyn. 38, 916–922 (2006). https://doi.org/10.1016/j.jct. 2005.10.004
- M.E. Mondéjar, J.J. Segovia, C.R. Chamorro, Improvement of the measurement uncertainty of a high accuracy single sinker densimeter via setup modifications based on a state point uncertainty analysis. Measurement 44, 1768–1780 (2011). https://doi.org/10.1016/j.measurement.2011.07.012
- 42. Lemmon EW, Bell IH, Huber ML, McLinden MO. NIST Standard Reference Database 23: Reference Fluid Thermodynamic and Transport Properties-REFPROP, Version 10.0. Natl Inst Stand Technol Stand Ref Data Progr 2018.
- 43. M.L. Huber, E.W. Lemmon, I.H. Bell, M.O. McLinden, The NIST REFPROP database for highly accurate properties of industrially important fluids. Ind. Eng. Chem. Res. 61, 15449–15472 (2022). https://doi.org/10.1021/acs.iecr.2c01427
- 44. GasCalc. Software for the calculation of physical natural gas properties, Version 2.8. SmartSim GmbH. Essen, Germany. 2024.
- D. Lozano-Martín, F. Pazoki, H. Kipphardt, P. Khanipour, D. Tuma, A. Horrillo, C. Chamorro, Thermodynamic (p, ρ, T) characterization of a reference high-calorific natural gas mixture when hydrogen is added up to 20 % (mol/mol). Int. J. Hydrogen Energy 70, 118–135 (2024). https://doi. org/10.1016/j.ijhydene.2024.05.028
- 46. D. Lozano-Martín, H. Kipphardt, P. Khanipour, D. Tuma, A. Horrillo, C.R. Chamorro, Impact of hydrogen addition, up to 20 % (mol/mol), on the thermodynamic (p, ρ, T) properties of a reference high-calorific natural gas mixture with significant ethane and propane content. Int. J. Hydrogen Energy 140, 256–271 (2025). https://doi.org/10.1016/j.ijhydene.2025.05.173
- 47. DIN. DIN EN 437:2021–07 Test gases Test pressures Appliance categories, Deutsches Institut für Normung e. V., Berlin, 2021.
- M. Farzaneh-Gord, B. Mohseni-Gharyehsafa, A. Toikka, I. Zvereva, Sensitivity of natural gas flow measurement to AGA8 or GERG2008 equation of state utilization. J. Nat. Gas Sci. Eng. 57, 305– 321 (2018). https://doi.org/10.1016/j.jngse.2018.07.014
- P. Ahmadi, A. Chapoy, B. Tohidi, Density, speed of sound and derived thermodynamic properties of a synthetic natural gas. J. Nat. Gas Sci. Eng. 40, 249–266 (2017). https://doi.org/10.1016/j.jngse. 2017.02.009

Publisher's Note Springer Nature remains neutral with regard to jurisdictional claims in published maps and institutional affiliations.

Authors and Affiliations

Daniel Lozano-Martín¹ · Dirk Tuma² · César R. Chamorro³

- César R. Chamorro cesar.chamorro@uva.es
- GETEF, Universidad de Valladolid, Valladolid, Spain
- ² BAM Bundesanstalt für Materialforschung und -Prüfung, Berlin, Germany
- MYER, Universidad de Valladolid, Valladolid, Spain

